Received: 19 February 2020 | Revised: 10 June 2020 | Accepted: 11 June 2020

DOI: 10.1002/ptr.6788

WILEY

RESEARCH ARTICLE

Piperlongumine inhibits head and neck squamous cell carcinoma proliferation by docking to Akt

Fei Lv[1] | Mingming Deng[2] | Jin Bai[1] | Dan Zou[1] | Jian Wang[3] | Hong Li[4] | Ye Zhang[1] | Xu Ji[5]

[1]The First Laboratory of Cancer Institute, The First Hospital of China Medical University, Shenyang, Liaoning, China

[2]Department of Respiratory and Infectious Disease of Geriatrics, The First Hospital of China Medical University, Shenyang, China

[3]Key Laboratory of Structure-Based Drug Design and Discovery of Ministry of Education, Shenyang Pharmaceutical University, Shenyang, China

[4]Department of Otorhinolaryngology Head and Neck Surgery, The Four Hospital of China Medical University, Shenyang, China

[5]Department of Otorhinolaryngology Head and Neck Surgery, The First Hospital of China Medical University, Shenyang, China

Correspondence
Xu Ji and Ye Zhang, No. 155 Nanjing North Street, Heping District, Shenyang, Liaoning Province, China.
Email: hljanterior@163.com (X. J.) and yzhang21@cmu.edu.cn (Y. Z.)

Funding information
National Natural Science Foundation of China, Grant/Award Number: 81270036; 30901736; 81802703; the Plan to Focus on Research and Development from Science and Technology project of Liaoning Province, Grant/Award Number: 2017225029

Piperlongumine (PL) is a biologically active alkaloid isolated from the long pepper roots and widely used as a traditional medicine in Ayurvedic medicine. However, the mechanism of PL's effect on head and neck squamous cell carcinoma (HNSCC) is not well understood. We performed cell experiments to confirm PL's inhibitory effect on HNSCC and employing cisplatin as positive control. Next, we conducted bioinformatics to predict PL's potential targets and verified by western blotting. Molecular docking, Biacore experiment and kinase activity assays were applied to elucidate the mechanism by which PL inhibited target activity. In vivo efficacy was verified by xenotransplantation and immunohistochemistry. PL inhibited proliferation, promoted late apoptosis, arrested cell cycle and inhibited DNA replication of the HEp-2 and FaDu cell lines. Employing bioinformatics, we found that PL's target was Akt and PL attenuated Akt phosphorylation. We found from molecular docking, Biacore experiment and kinase activity assay that PL inhibited Akt activation by docking to Akt to restrain its activity. In addition, PL significantly inhibited the growth of xenograft tumors by down regulating the expression of p-Akt in vivo. This study provides new insights into the molecular functions of PL and indicate its potential as a therapeutic agent for HNSCC.

KEYWORDS
Akt, bioinformatics, HNSCC, molecular docking, Piperlongumine

1 | INTRODUCTION

Head and neck squamous cell carcinoma (HNSCC) accounts for 5% of the malignant tumors in the whole body, and there are about 650,000 new cases in the world every year (Dubal et al., 2016). Moreover, due to the special anatomical location, HNSCC seriously affect the survival and quality of life of patients (Cancer Genome Atlas Network, 2015). Surgery, radiotherapy, chemotherapy and target therapy (Massard et al., 2016) are the conventional treatment methods for HNSCC, but the effect is limited and has a lot of side effects. Complications such as fistula and cachexia also affect the quality of life of HNSCC patients (Simon & Caballero, 2018). Therefore, it is very necessary to find more safe and effective alternative treatment drugs for HNSCC.

Piperlongumine (PL) is a kind of small molecular amides with biological activity extracted from *Piper nigrum*, which is one of the most commonly, used herbal medicines. Previous studies have shown that PL has a killing effect on ovarian cancer, colorectal cancer and other cancers (Chen, Lian, Yuan, & Li, 2019; Gong et al., 2014). In addition, PL is also combined with cisplatin, doxorubicin and other chemotherapy drugs to treat cancers (Chen, Lian, et al., 2019; Chen et al., 2019; Seber, Sirin, Yetisyigit, & Bilgen, 2020). Mechanically, PL can selectively kill cancer

cells by increasing Reactive Oxygen Species (ROS) levels in many malignant cells (Karki, Hedrick, Kasiappan, Jin, & Safe, 2017; Thongsom, Suginta, Lee, Choe, & Talabnin, 2017; Zhou, Huang, Ni, & Lv, 2020). In addition, cell cycle arrest is one of the mechanisms by which PL kills cancer cells (Seok et al., 2018). Other studies (Liu et al., 2018; Yamaguchi, Kasukabe, & Kumakura, 2018) showed that PL induced ferroptosis and autophagy, suggested that PL can cause cell death in many ways. Studies have shown that various derivatives of PL also have anti-tumor effects (Li et al., 2019). In addition, PL also has therapeutic effects on neurodegenerative (Gu et al., 2018) and inflammatory diseases (Lu et al., 2019). However, the effect and mechanism of PL on HNSCC, especially laryngeal and hypopharyngeal cancers have not been reported.

Malignant tumors are the result of multiple signaling pathways. Akt consists of three conserved domains, including an N-terminal pleckstrin homology, a central catalytic kinase domain, and a C-terminal domain (Calleja et al., 2007). Abnormal activation of PI3K/Akt signaling pathway participates in various tumorigeneses. When receptor tyrosine kinase (RTKs) and G protein coupled receptor (GPCR) are activated by external signals, PI3K recruits serine/threonine kinase (Akt) from the cytoplasm and transports it to the membrane, and phosphorylates serine phosphorylation site (ser473) and threonine phosphorylation site (thr308) of Akt to activate it. The activated Akt is imported into the nucleus, activates or inhibits a variety of downstream proteins such as mammalian target of rapamycin (mTOR), and participates in the regulation of cell proliferation, apoptosis and angiogenesis (Jiang & Liu, 2008; Mayer & Arteaga, 2016). Akt expression is associated with the prognosis of many tumors including HNSCC (Garcia-Carracedo et al., 2016). Akt inhibitors include: AZD5363 (Robertson et al., 2019), GDC-0068 (Ippen et al., 2019) etc. Most of them are ATP-competitive, which binds to the catalytic kinase domain competively (Bhutani, Sheikh, & Niazi, 2013), and the existing Akt inhibitors have not been reported to be effective in HNSCC treatment.

In this study, we explored the anti-cancer roles of PL in vitro and in vivo and the PL target was predicted and verified by network pharmacology and computer aided drug design (CADD). PL inhibited Akt activity by binding directly to Akt, which was the mechanism of PL in the treatment of HNSCC. The study showed PL may be a promising adjuvant therapy for HNSCC.

2 | MATERIALS AND METHODS

2.1 | BATMAN-TCM

BATMAN-TCM (Bioinformatics Analysis Tool for Molecular mechANism of Traditional Chinese Medicine, http://bionet.ncpsb.org/batman-tcm/) is an online bioinformatics database designed for traditional herbal medicines molecular mechanism study. It is an online pharmacological analysis tool based on the target prediction of traditional herbal ingredients and potential drug targets (Liu et al., 2016). PubchemCompound database (https://www.ncbi.nlm.nih.gov/pccompound/) in NCBI is a database of organic small molecules biological activity, which is a database of chemical modules and contains description information of compounds. In this study, we obtained the PubChem CID (637858) of PL through NCBI PubChem compound database, submitted it to the BATMAN-TCM database, set the score cutoff to 20, Adjusted *p*-value to .05, and obtained the target.

2.2 | TCMSP

TCMSP (Traditional Chinese Medicine Systems Pharmacology, http://lsp.nwu.edu.cn/tcmsp.php), the pharmacology database and analysis platform of traditional medicine system, through text mining and database integration, obtained the basic information of pharmacokinetics and drug target protein network of 30,069 traditional medicine compounds (Ru et al., 2014). We input the CAS number of PL (20069–09-4) obtained from PubchemCompound database into the TCMSP database to obtain the target of PL. The drug target name is corrected to the Official Symbol by the UniProtKB search function in the UniProt database (https://www.uniprot.org/).

2.3 | Comparative toxicogenomics database

CTD (Comparative Toxicogenomics Database, http://ctd.mdibl.org/) is a robust, publicly available database that aims to advance understanding about how environmental exposures affect human health. It provides manually curated information about chemical-gene/protein interactions, chemical-disease and gene-disease relationships. These data are integrated with functional and pathway data to aid in development of hypotheses about the mechanisms underlying environmentally influenced diseases (Davis et al., 2009). We used CTD's Chemicals-Genes Interaction search panel and input “Piperonumine” to get the target of PL.

2.4 | Gene ontology term analysis and kyoto encyclopedia of genes and genomes pathways analysis

Gene ontology (GO) functional annotation (Ashburner et al., 2000) and Kyoto Encyclopedia of Genes and Genomes (KEGG) pathway analysis (Kanehisa & Goto, 2000) of the PL-related targets were performed using DAVID 6.7 database (https://david.ncifcrf.gov/home.jsp) (Huang, Sherman, & Lempicki, 2009). Biological processes (BP), molecular functions (MF), and cellular components (CC) of the target were visualized using the ggplot2 package in R 3.5.3.

2.5 | Genecards

Genecards database (https://www.genecards.org/) provides concise genomes, proteomes, transcriptions, genetics, and functions of all known and predicted human genes. We obtained HNSCC target through Genecards database.

2.6 | Cytoscape

Cytoscape software is a tool for visualizing biological networks composed of proteins and drugs, with functions of editing and analyzing biological molecular networks (Saito et al., 2012). The obtained PL related targets were intersected with HNSCC related targets, and Cytoscape 3.6.1 software was used to construct drug target network. We used the Network Analyzer plugin to analyze the topology of the network. Degree, Betweenness and Closeness centrality are important parameters in network pharmacology analysis. According to previous studies (Ke et al., 2019), genes with higher-degree distributions in the regulatory network play an important role in the treatment of PL, so we selected the target with the highest degree as the core target.

2.7 | Molecular docking

Docking was performed by Schrödinger, including module of Protein Preparation Wizard, LigPrep, and Glide. Akt crystal structure (PDB ID: 6CCY) (Ashwell et al., 2012) was prepared from RCSB (Burley et al., 2019) and optimized with the Protein Preparation Wizard. Combining with previous reports, LigPrep was used to generate multiple conformational states of ligand molecules for PL. Docking between PL and Akt in SP (standard precision) was performed by Glide (Friesner et al., 2004; Halgren et al., 2004). We validated docking model through redock approaches according to previous researches (Yadav, Dhawan, et al., 2014; Yadav, Kalani, et al., 2014; Yadav, Kalani, Khan, & Srivastava, 2013). The root-mean-square deviation (RMSD) value was calculated from superimposed ligands to examine docking parameters that were capable of reproducing a similar conformation to that of the co-crystal at the active site of Akt. The interactions were visualized by PyMOL (PyMOL Molecular Graphics System, Schrodinger LLC, New York, NY).

2.8 | Biacore assay for surface plasmon resonance analysis

Surface plasmon resonance (SPR) affinity experiment (Leonard, Hearty, Ma, & O'Kennedy, 2017) for drug-target interaction analysis was conducted employing a Biacore 100 T biosensor detector (GE healthcenter, USA). Different concentrations of PL was injected to protein (Human Akt1 Protein, His, Strep II Tag Protein [AK1-H5283]) and blank channels. The experiment was conducted at 25°C, the supernatant flow rate was 20 μl/min. 10 mM acetate was employed as immobilization buffer and 1xPBS as running buffer.

2.9 | Akt kinase enzymatic assay

Akt kinase enzymatic assay was conducted by the Kinase Activity Assay Kit (Abace, Beijing, China) following the manufacturer's protocol. Purified human Akt protein was administrated with different concentrations of PL in a black 384-well plate. The fluorescence intensity was measured by an automatic microplate reader.

2.10 | Cell lines and reagents

Human HNSCC cell lines HEp-2 (laryngeal cancer cell line) and FaDu (hypopharyngeal cancer cell line) were purchased from the Cell Bank of Type Culture Collection of the Chinese Academy (Shanghai, China). These two cell lines were cultured in RPMI 1640 (Bioind) with 10% fetal bovine serum (Bioind) and were kept in an incubator at 37°C with 5% CO_2.

PL was purchased from Sigma-Aldrich (528124). We added 1,577 μl DMSO into 5 mg PL to prepare 10 mM PL storage solution. SC79, an Akt activator, was also purchased from Sigma-Aldrich (123871). 6,868 μl of DMSO dissolves SC79 powder to prepare 10 mM SC79 storage solution. Cisplatin (cDDP), a positive control reagent, was bought from Sigma-Aldrich (P4394). We measured 6 mg cDDP, added 2 ml DMSO, and dissolved into 10 mM cDDP storage solution. All of the storage solution were storeged in the −20°C and fresh medium dilutions were prepared for each experiment.

2.11 | MTT

Cell viability was examined using the MTT (3-[4,5-dimethylthiazol-2-yl]-2,5-diphenyltetrazolium bromide) assay. Cells (5,000 cells/well) were seeded in a 96-well plate overnight before exposed to different concentrations of PL (or cDDP) and incubated for another 24 or 48 hr. 20 μl of MTT solution (5 mg/ml, Sigma, M5655) were added into each well and the cells were incubated for next 4 hr at 37°C. The supernatant was then removed and 200 μl of DMSO were added to each well to dissolve the precipitate. Absorbance was measured by a spectrophotometer (BIOBASE, EL10A) at 490 nm.

2.12 | Colony formation

Cells were seeded in six-well plates at a density of 1,200 cells/well. On the second day, cells were treated with different concentration of PL (or 10 μM cDDP).

Seven days after the feeding, cells were fixed with absolute ethanol for 20 min and then stained with 0.1% crystal violet. Finally, stained cell colonies were photographed with a digital camera and analyzed using ImageJ (National Institutes of Health [NIH], Bethesda, USA).

2.13 | Flow cytometry

Cells cultured in a six pore plate and administrated with different concentrations of PL (or 10 μM cDDP) for various time points were collected and incubated with 10 μl of Propidium Iodidec (PI) and 5 μl of Annexin V for 15 min in the dark. The samples were then assessed

using flow cytometry and the data were analyzed using FlowJo (Version X; TreeStar, Ashland, OR).

2.14 | EdU staning

To make sure the effect of PL on cell proliferation of HEp-2 and FaDu cells, we determined the DNA replication induced by PL through EdU/Apollo488 staining (Ribobio, C10301-1). EdU staining was conducted as manufacturer's protocal. Briefly, cultured HNSCC cells treated with 10 μM PL or cDDP were exposed to EdU (50 μM) for 3 hr, then fixed with 4% paraformaldehyde and permeabilized with 0.4% Triton X-100. Cells were washed by PBS three times, and then incubated with Apollo488 staining cocktail in dark at room temperature for 30 min and counterstained with 1xHoechst 33,342 for another 30 min. Images were acquired by fluorescence microscope and analyzed by ImageJ.

2.15 | Western blotting

Proteins treated with different concentration of PL, with or without SC79 (Akt phosphorylation activator), were extracted from the cells and quantified. Equal amounts of protein were separated by electrophoresis on sodium dodecyl sulfate polyacrylamide gels and transferred to polyvinylidene fluoride membranes. The membranes were blocked with 5% non-fat milk in TBST (10 mM Tris–HCl, pH 7.4, 100 mM NaCl, 0.5% Tween-20) for 40 min at room temperature and incubated overnight at 4°C with primary antibodies (p-Akt et al. Cell Signaling Technology, 4,060). The membranes were then washed in TBST and incubated with secondary antibodies (zsbio, ZB-2301) for 40 min. After extensive washing, membranes were visualized using the enhanced chemiluminescence reagent. Final images were analyzed using ImageJ.

2.16 | In vivo experiments

We acquired 4–6 weeks BALB/c nude mice from the National Laboratory Animal Center (Shanghai, China) after obtaining appropriate institutional review board permission and raised in a pathogen-free environment. Each nude mouse was injected subcutaneously in the flank with $5 * 10^6$ FaDu cells. When the tumor volume reached approximately 60 mm^3, mice were randomly assigned to the vehicle control (saline) or PL alone (five animals in each group) groups. The PL group was administered with 500 μL of solution containing 0.2 mg of PL. Drugs were administered by intraperitoneal injection (i.p.) once every 2 days. Tumor volume was calculated using the following equation: volume = $(width^2 * length)/2$. After 21 days, mice were sacrificed and their xenografts were removed for immunohistochemical staining. All animal experiments were conducted under a protocol approved by the Ethics Committee of the First Affiliated Hospital of China Medical University.

2.17 | Immunohistochemistry

Formalin-fixed tissues were embedded in paraffin and cut into 5-μm thick sections for H&E staining and immunostaining. The expression levels of p-Akt and Ki-67 were assessed using the immunohistochemical staining kit (Maixin, China). De-waxed sections were washed in PBS and exposed to 3% H_2O_2 for 15 min at room temperature to quench the endogenous peroxidase activity. Then the tissues were blocked with normal goat serum for 20 min at room temperature. After incubation with primary antibody (1:100) overnight at 4°C, tissues were incubated with the secondary antibody and biotin-labeled horseradish peroxidase. Subsequently, antibody binding was visualized using a 3,3′-diaminobenzidine tetrahydrochloride (DAB) kit (Maixin, China) before brief counterstaining with hematoxylin. Eventually, tissues were gradually dehydrated, sealed with neutral gum, observed, and photographed with an inverted phase contrast microscope.

Immunoreactivity was semi-quantitatively evaluated and evaluated by a pathologist (Wanying Huang, Department of Pathology, Shengjing Hospital of China Medical University). Five representative regions were randomly selected from the 400-fold field of view of the microscope. The score of each field of view was determined by the proportion of positive cells and the color rendering intensity. According to the proportion of positive cells: <5, 5–25, 25–50, 50–75, 75–100%, the scores of 0, 1, 2, 3, and 4 were obtained respectively. According to the intensity of coloring, 0, 1, and 2 points were obtained for uncolored, yellow and brown respectively. The final score was obtained by multiplying the scores of the two items and taking the average score of the five visual fields.

2.18 | Statistical methods

Results were analyzed using the SPSS software (SPSS, Chicago, IL). All experiments were independently repeated at least three times and data were presented as the mean ± SD and standardized. Student's two-tailed *t*-test and one-way ANOVA were performed to determine statistical significance between PL and control groups. Differences were considered significant when *p*-values <.05.

3 | RESULT

3.1 | The function of PL on proliferation, apoptosis and cell cycle in HNSCC cells

The inhibitory role of PL on HNSCC cells proliferation was investigated by MTT, colony formation, flow cytometry, cell cycle genes expression and EdU staining. The MTT assay showed obviously less proliferation with the treatment of PL, in a time- and concentration-dependent manner (IC_{50}: HEp-2:24 hr: 15.97 μM, 48 hr: 4.34 μM. FaDu: 24 hr: 10.27 μM, 48 hr: 7.12 μM. Figure 1A). And as illustrated in Figure 1B, cell colony numbers significantly reduced in PL treatment group. We determined whether PL causes changes in the

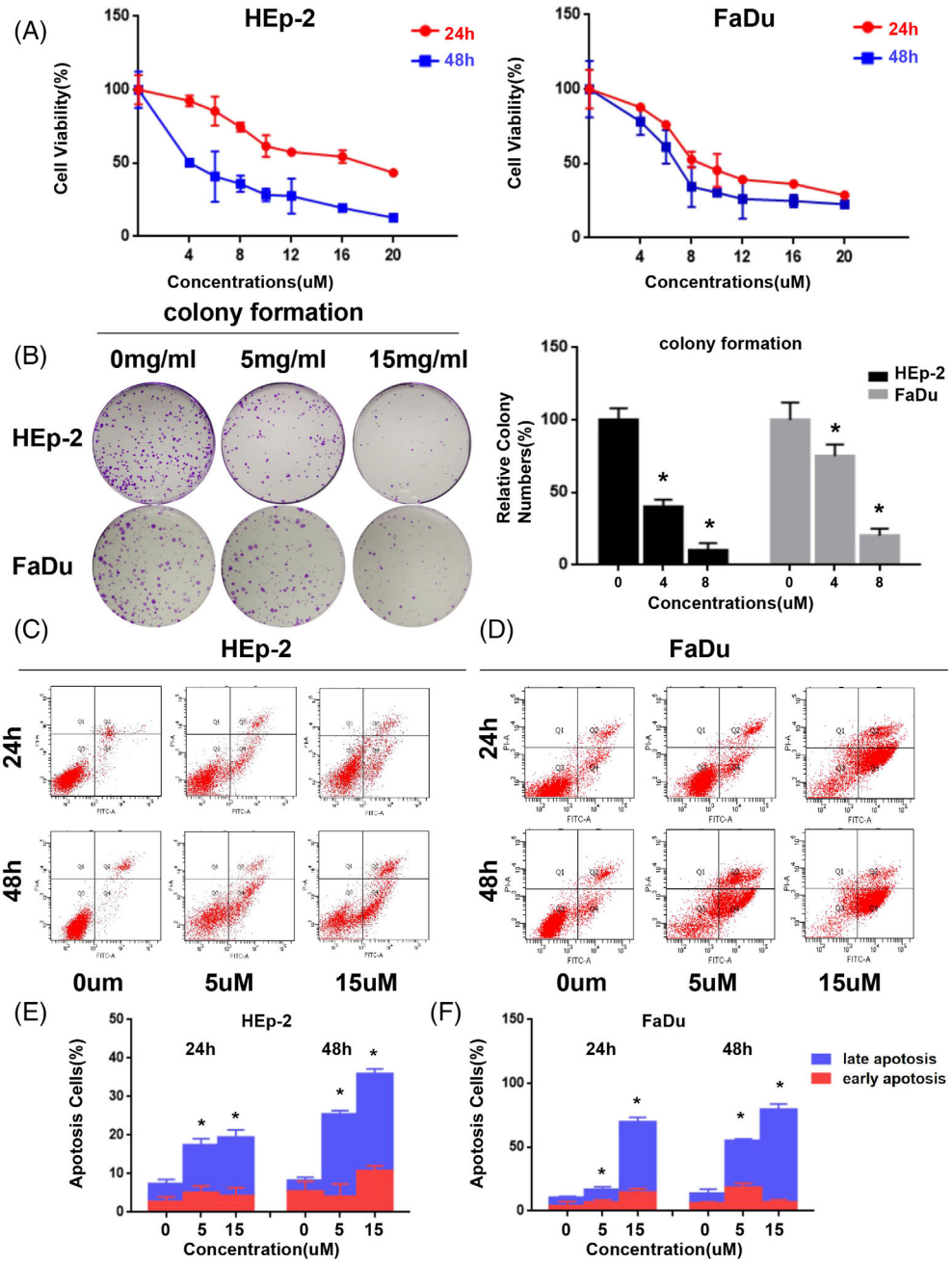

FIGURE 1 PL inhibited HNSCC cell lines proliferation in vitro. (A) Concentration- and time- dependent inhibitory effect of PL on HNSCC cell lines. HNSCC cell lines (HEp-2 and FaDu) were administrated with PL and the cell viability was analyzed by MTT assay. (B) PL inhibited the colony formation significantly on HNSCC cell lines. Cells were treated with different concentrations of PL and the colony formation was analyzed. Data represents mean ± SD, $^*p < .05$. (C and D) Flow cytometry analysis. Cells were treated with different concentrations of drugs for 24 and 48 hr and apoptosis test of flow cytometry was performed as described. Apoptotic intensity was measured by flow cytometry and analyzed by flowjo. (E,F) Quantification of the apoptosis rate by histogram. Data represents mean ± SD, $^*p < .05$, two cell line experiments ($n = 2$) were repeated three times independently [Colour figure can be viewed at wileyonlinelibrary.com]

numbenr of apoptotic cell by flow cytometry. PI-annexin V staining showed that apoptotic cells increased (upper right quadrant: early apoptosis, lower right quadrant: late apoptosis) and that PL promoted both early and late apoptosis (total apoptosis rate: HEp-2 24 hr: 0 μM: 7.3 ± 2.5%, 5 μM: 15.4 ± 3.5%, 15 μM: 19.4 ± 4.4%; 48 hr: 0 μM: 8.2 ± 3.5%, 5 μM: 25.4 ± 4.3%, 15 μM: 35.9 ± 2.7%. FaDu 24 hr: 0 μM: 10.4 ± 3.1%, 5 μM: 16.6 ± 3.2%, 15 μM: 69.5 ± 4.6%. 48 hr: 0 μM: 13.6 ± 2.2%, 5 μM: 55.0 ± 4.8%, 15 μM: 79.4 ± 3.8%, Figure 1C–F). Cell cycle analysis revealed that administration of PL resulted in increasing of S phase (S phase rate: HEp-2 0 μM: 9.98 ± 2.2%, 5 μM: 20.3 ± 5.9%, 15 μM: 37.56 ± 11.0%. FaDu 0 μM: 11.43 ± 3.6%,5 μM: 28.72 ± 7.8%, 15 μM: 41.13 ± 12.4%, Figures 2A,B and S1A). Furthermore, the effect of PL on the expression level of cell cycle-associated genes, CDK1 and Cyclin B1 gene expression were examined. The results showed that PL decreased the protein level of the two cell cycle-associated genes (Figures 2C,D and S1B). At last, the anti-proliferative activities of PL against HNSCC cell lines were examined by the EdU assay. As shown in Figures 2E,F and S1C-D, PL suppressed DNA replication. To sum up, these results demonstrated that PL inhibited the proliferation of the HNSCC cells.

3.2 | Evaluation of PL cytotoxicity

In order to further evaluate the inhibitory effect of PL on the growth of HNSCC cells, we selected cDDP, the first-line chemotherapy drug

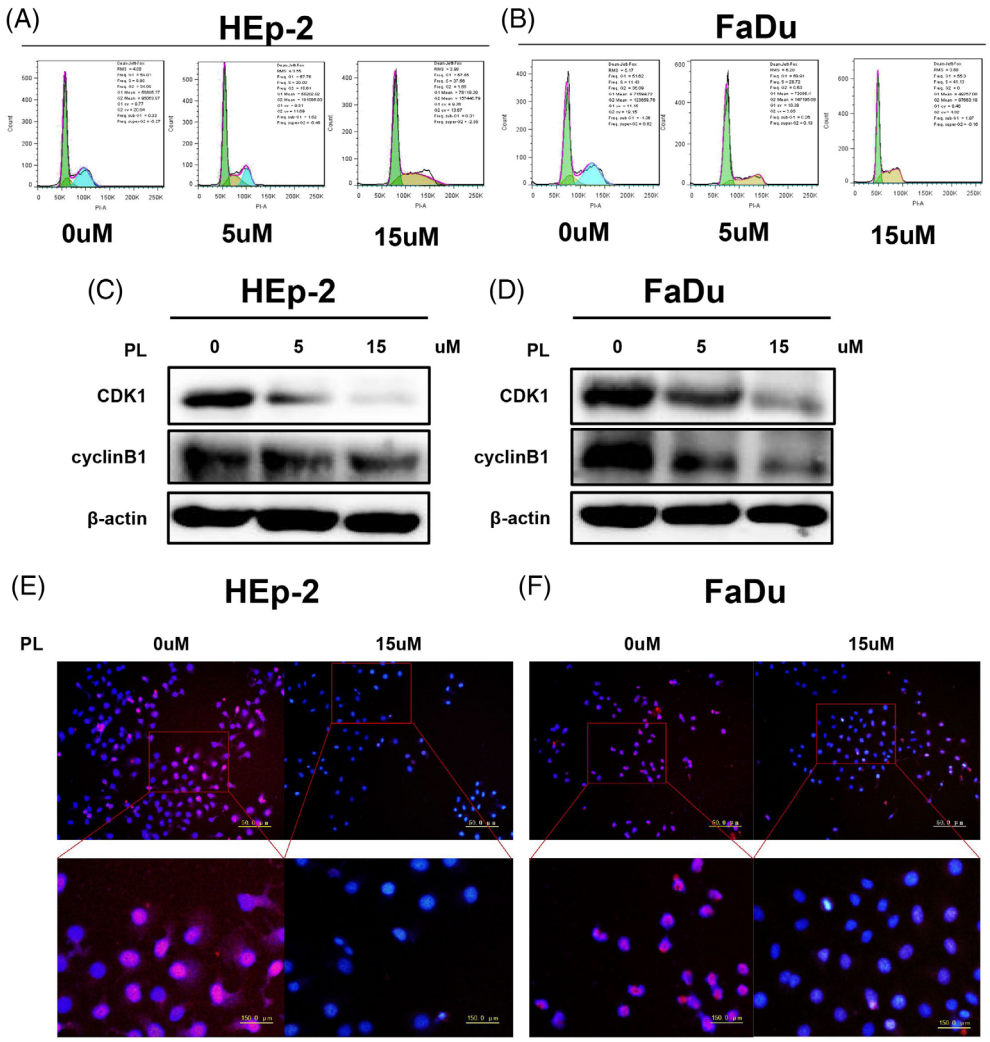

FIGURE 2 PI induced HNSCC cell cycle arrest. (A and B) Effect of PL on S phase population in HNSCC cell lines. Cells were treated with different concentrations of drugs for 24 hr. Cell cycles were analyzed by flow cytometry as described in the materials and methods section. (C and D) Western blot analysis of total-cell extracts of HNSCC cell lines treated with PL to evaluate the effect of PL on cell cycle. Markers of cell cycle, including CDK1 and cyclinB1, were measured by western blotting. β-Actin was used as internal control. (E and F) EdU staining assay was performed to detect DNA replication in HNSCC cells. EdU positive cells was stained red and the nuclei were stained blue. The scale bars indicated 50 μm/150 μm. Two cell line experiments (n = 2) were repeated three times independently [Colour figure can be viewed at wileyonlinelibrary.com]

of HNSCC (Hutchinson, 2016) as the standard reference drug. The results of MTT showed that PL and cDDP had similar inhibitory effect on HNSCC cell proliferation at low concentration (5–10 uM), but at high concentration (20–30 uM), the cytotoxicity of PL was weaker than that of cDDP (Figure 3A). Combined with previous research (Bostan et al., 2019; Xue et al., 2019), we selected the concentration of 10 uM to further evaluate the effect of PL through other proliferation-related experiments. In the colony formation experiment, PL and cDDP inhibited colony formation to a similar extent (Figure 3B). By PI annexin V staining, we found that both PL and cDDP promoted early and late apoptosis, without statistic difference (total apoptosis rate: HEp-2:0 μM: 3.3 ± 0.91%, PL: 14.7 ± 2.6%, cDDP: 14.5 ± 2.5%; FaDu: 0 μM: 3.6 ± 1.0%, PL 18.4 ± 2.3%, cDDP: 21.6 ± 2.6%. Figures 3C,D and S2A). In EdU staining, after adding PL or cDDP, EdU positive cells decreased, and both drugs could inhibit DNA replication, and the DNA replication inhibition of cDDP is more significant (Figures 3E,F and S2B). On the one hand, the proliferation inhibition of PL is not inferior to that of standard reference drug cDDP. On the other hand, due to the high tolerance of PL, we think PL is still a promising anti HNSCC drugs.

3.3 | PL target prediction based on network pharmacology

Through the BATMAN-TCM, TCMSP and CTD databases, we obtained a total of 59 possible targets (Table 1). In order to further deepen the understanding of target proteins, we used the R ggplot package for GO function and KEGG pathway enrichment analysis. The result is shown in Figure 4A–C, Integral Component of Plasma Membrane was the most significant Cellular Component (CC) term, and G-protein Coupled Acetylcholine Receptor Activity was the most significant Molecular Function (MF) term. KEGG pathway shows that the targets were involved in cGMP-PKG signaling pathway (Figure 4D). The results of GO function and KEGG Pathway analysis indicate that PL's target may be involved in intracellular signaling. In the GeneCards database, we obtained 3,897 HNSCC-related targets, and 59 PL targets were intersected with HNSCC-related targets. A total of 41 possible targets (Figure 4E) of PL inhibition HNSCC were obtained. We input these 41 targets into Cytoscape3.6.1 and obtained the drug target Network Map (Figure 4F). Network Analyzer is used for topology analysis, and Degree is taken as the screening condition of important target genes.

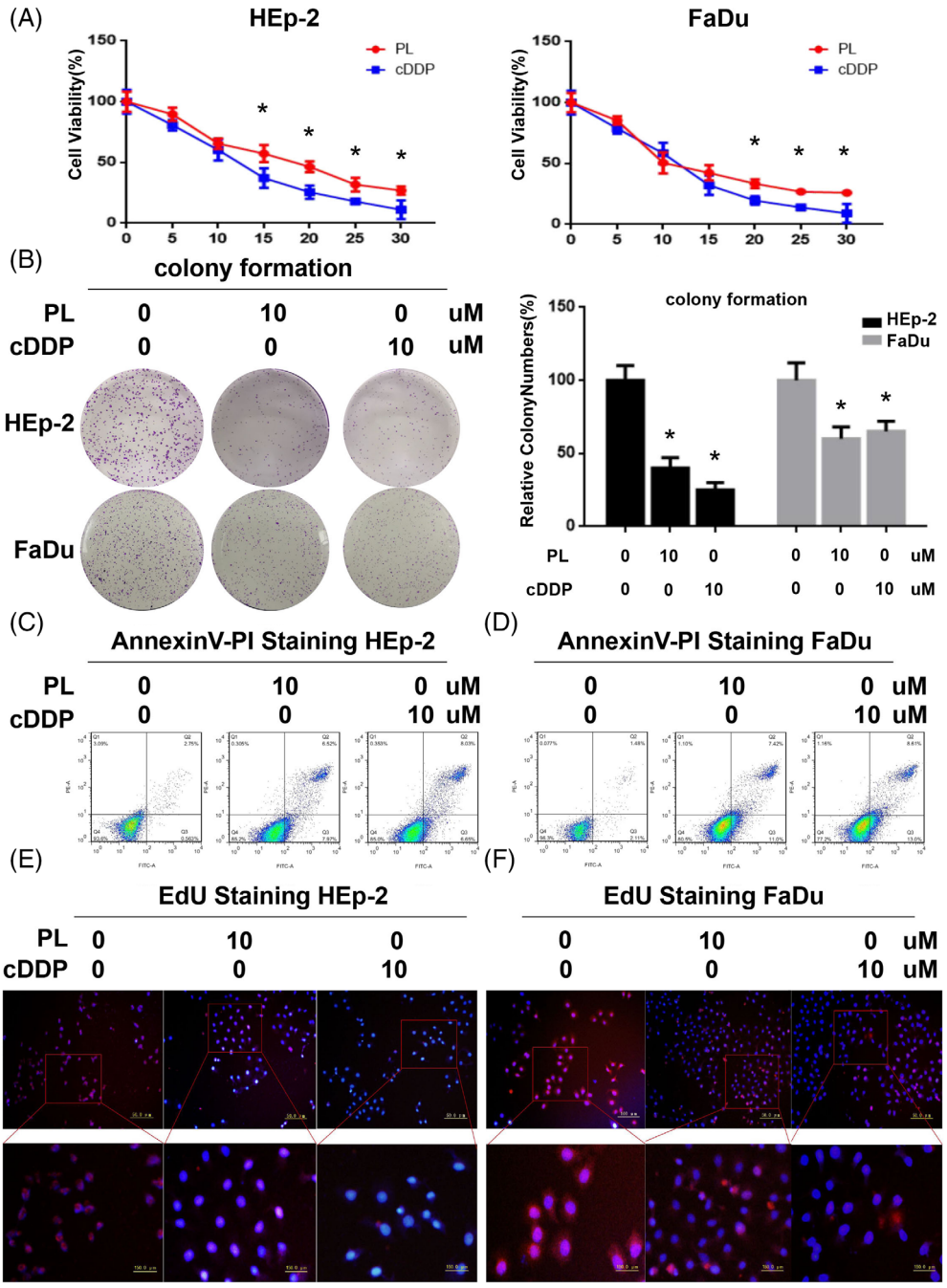

FIGURE 3 Evaluation of PL cytotoxicity. (A) MTT analysis of HNSCC cell viability treated by PL or cDDP. The proliferation inhibitory of the two drugs was compared. (B) PL and cDDP inhibited colony formation of HNSCC cells similarly. (C,D) Analysis of apoptotic cell portion induced by PL or cDDP was performed by flow cytometry. (E,F) DNA replication induced by PL or cDDP was detected by EdU staining. EdU positive cells was stained red and the nuclei were stained blue. The scale bars indicated 50 μm/150 μm. Two cell line experiments (n = 2) were repeated three times independently [Colour figure can be viewed at wileyonlinelibrary.com]

Akt1 with the highest Degree (Degree = 29) is the core target gene. Therefore, we hypothesized that PL inhibits HNSCC by Akt.

3.4 | PL docks to Akt

Next, we applied western blot to detect the inhibition of PL on Akt activation. HNSCC cell lines (HEp-2, FaDu) were treated with different concentrations of PL for 24 hr to extract total protein. The results showed that the expression of total-Akt was unchanged, while the expression of phospho-Akt (Ser 473) was down regulated (Figures 5A and S2C,D). SC79 is a novel, selective, highly-efficient, and small-molecule Akt activator (Zhu et al., 2019). When we treated both PL (10 μM, 24 hr) and SC79 (10 μM, 1 hr) with HEp-2 and FaDu cells, PL inhibited SC79-induced Akt activation (Figures 5B and S2E,F). These results indicate that PL can inhibit Akt activation. Previous studies have shown that PL attenuates Akt activation by inhibiting PI3K pathway (Kumar & Agnihotri, 2019; Wang et al., 2018). In order to explore other possible mechanisms of PL inhibiting Akt, we conducted molecular docking between PL and Akt. Molecular docking predicts potential interactions of the proposed protein with the selected molecule, which is a structural modeling approach to study possible binding sites for cancer therapeutics. AZD5363 (Davies et al., 2012) was chosen as positive control to investigate the energy matching and geometrical complementarity of

TABLE 1 PL targets predicted by bioinformatics

Database	Predicted targets				
BATMAN-TCM	PDE3A	PDE3B	ADRA1A	ADRA2A	KCNH6
	GGCX	ADRA1D	F10	KCNH2	PTGS1
	ADRA1B	PTGS2	KCNH7	ADRA2B	PDE5A
	SIRT2	HCN4	AURKA	SLC6A4	RAPGEF2
	PDE2A	HCN2			
TCMSP	NOS2	PTGS1	DRD5	CHRM3	CHRM1
	SCN5A	CHRM5	PTGS2	NOS3	CHRM4
	RXRA	PDE3A	ADRA1A	CHRM2	ADRA1B
	PTPN1	SLC6A3	ADRB2	SLC6A4	OPRM1
	GABRA1	HSP90	LTA4H	PRKACA	CAMKK2
CTD	Akt1	BAX	CASP3	CBR1	CCND1
	CDK4	CDK6	CDKN1A	FOXO1	MAPK1
	MAPK3	NFKBIA	PARP1	RB1	RELA
	TP53	TP73	XPO1		

the PL and the crystal structure of Akt. PL has similar Akt binding capacity with AZD5363 (Docking Score: PL = −4.691 kcal/mol, AZD5363 = −6.000 kcal/mol). As shown in Figure 5C, PL and AZD5363 form hydrogen bonds with the negatively charged residues of Akt, suggesting that PL and AZD5363 may have similar effects on Akt. Binding of PL to Akt showed a canonical hinge interaction. For the ligand crystal (PL), the 5,6-dihydropyridin-2(1H)-one extended deeper into the kinase active site whereas the 1,2,3-trimethoxybenzene extended toward solvent. The carbonyl oxygen forms hydrogen bond, which is an essential group of drugs. Next the molecular docking was evaluated by redocking poses of crystal structure and calculating RMSD. The docking method was considered accurate while the confirmation RMSD value calculated was less than 2.0 Å (Nguyen et al., 2016). The RMSD value of the poses obtained by docking methods was 1.781 Å (Figure 5D) and the docking could be thought accurate. Figure S3A,B shows the combination of PL and Akt pockets: PL and Akt combine well without significant steric hindrance. When we performed a Biacore experiment, with the increasing of PL concentration, positive signals became more significant. PL directly binds to Akt in a concentration-dependent manner and has micromolar binding affinity (K_D = 123.3 μM, Figure 5E and S3C). Next, we verified the conclusion by kinase activity assay: PL inhibits Akt kinase activity with IC_{50} of about $1.115 * 10^{-7}$ M (0.1115 μM, Figure 5F). To sum up, PL docks to Akt to inhibit its activition.

3.5 | PL inhibits HNSCC by attenuating Akt activation in vivo

Human HNSCC xenotransplantation model with FaDu cells was used to validate cell experimental results. PL was administered for 22 days before the mice were sacrificed and tumor nodules were observed. Xenograft tumor volume was decreased after PL administration compared to the control group (Figure 6A). The size of transplanted tumors was regularly monitored during drug administration. The growth rate of transplanted tumors in the PL treatment group was slower than that in the control group. There was a significant difference in the size of transplanted tumors after about 19 days (Figure 6B). The weight of xenograft tumors was also significantly lower than that of the control group. The average weight of xenograft tumors in the PL treatment group was 0.4 ± 0.05 g and 0.76 ± 0.15 g in the control group (Figure 6C). To further explore the mechanism of PL on tumor growth inhibition, p-Akt and cell proliferation marker Ki-67 expression levels were detected using immunohistochemistry. We observed that the transplanted tumor was multinodular growth and p-Akt was mainly expressed on the lateral side of tumor mass. PL reduced the immunohistochemical scores of p-Akt and proliferation marker Ki-67 (Figure 6D and S3D). These results demonstrated that PL is effective in vivo.

4 | DISCUSSION

Laryngeal squamous cell carcinoma (LSCC) originates from the human mucosal epithelium of the larynx, accounting for 5.7–7.6% of systemic malignancies (Steuer, El-Deiry, Parks, Higgins, & Saba, 2017). Hypopharyngeal cancer is a malignant tumor of the head and neck, one of the most malignant tumors of the upper digestive tract and upper respiratory tract, which mechanism is not clear (Kuo et al., 2016). The main reasons of poor prognosis include local recurrence, prone to lymph node metastasis and distant metastasis, and lack of effective drug therapy (Kaidar-Person, Gil, & Billan, 2018). Therefore, it is of great significance to search for drugs for HNSCC replacement therapy to improve the prognosis of HNSCC.

PL is a plant derived compound that has been shown to have a broad spectrum of antitumor effects (Farooqi et al., 2018). It has been reported that PL selectively induces cancer cells death and delays tumor growth in hematologic tumor (Han, Han, & Kamberos, 2014; Han, Son, Yun, Kamberos, & Janz, 2013) and solid tumor (Wang, Mao, You, Hua, & Cai, 2015). In the study of herbal medicine, investigation

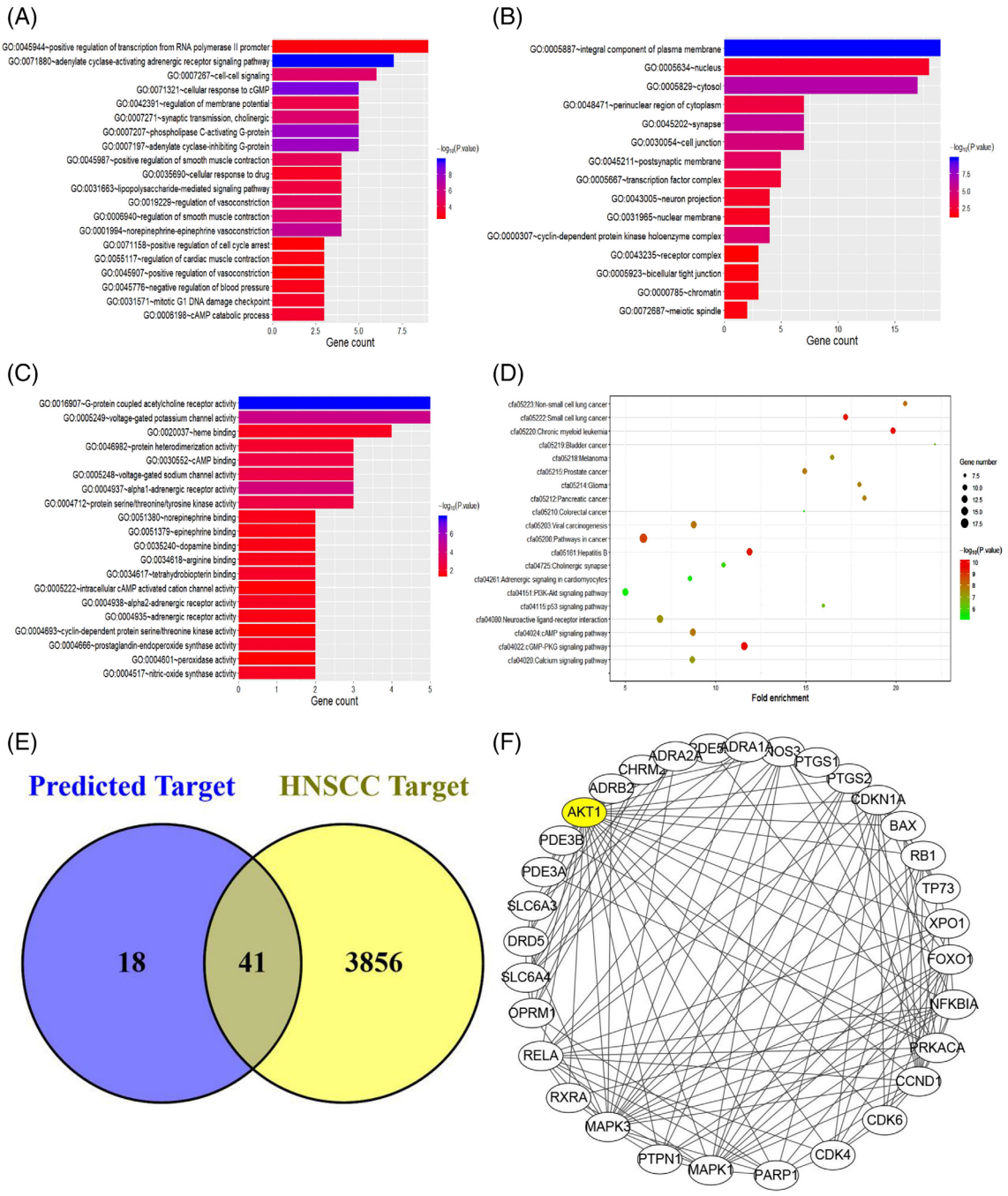

FIGURE 4 Bioinformatics prediction of PL targets. (A–C) Gene Ontology (GO) term enrichment analysis of PL targets, with the domains of biological processes (BP, A), cellular components (CC, B), and molecular functions (MF, C). The length of bars presented the gene counts and the gradation of color stood for the value of minus log10 adjusted P value. (D) KEGG pathway enrichment analysis of PL targets with the top 20 enrichment scores. The size of the dot presented the gene counts; the gradation of color stood for the value of minus log10 *P* value. (E) Identification of PL's targets on HNSCC in public drug databases and GeneCards. (F) Network of PL targets protein–protein interaction. PPI network was composed of 59 nodes (PL targets) and 295 edges [Colour figure can be viewed at wileyonlinelibrary.com]

of mechanisms using bioinformatics can provide new research directions and ideas for traditional experimental research methods (Xue et al., 2013). Akt may be a target for PL, as predicted by network pharmacology and verified by western blot. Molecular docking can simulate drug-target binding by energy and space matching between receptors and ligands (Wang & Yu, 2018). Through molecular docking, Biacore test and kinase activity assay, we believe PL can inhibit the activation of Akt by directly docking to Akt. These results suggest the therapeutic potential of PL in HNSCC cancer patients.

Recent studies have identified the multiple molecular targets of PL that may have a role in cancer therapy, include kinases, transcription factors, and growth factors and their receptors, among other

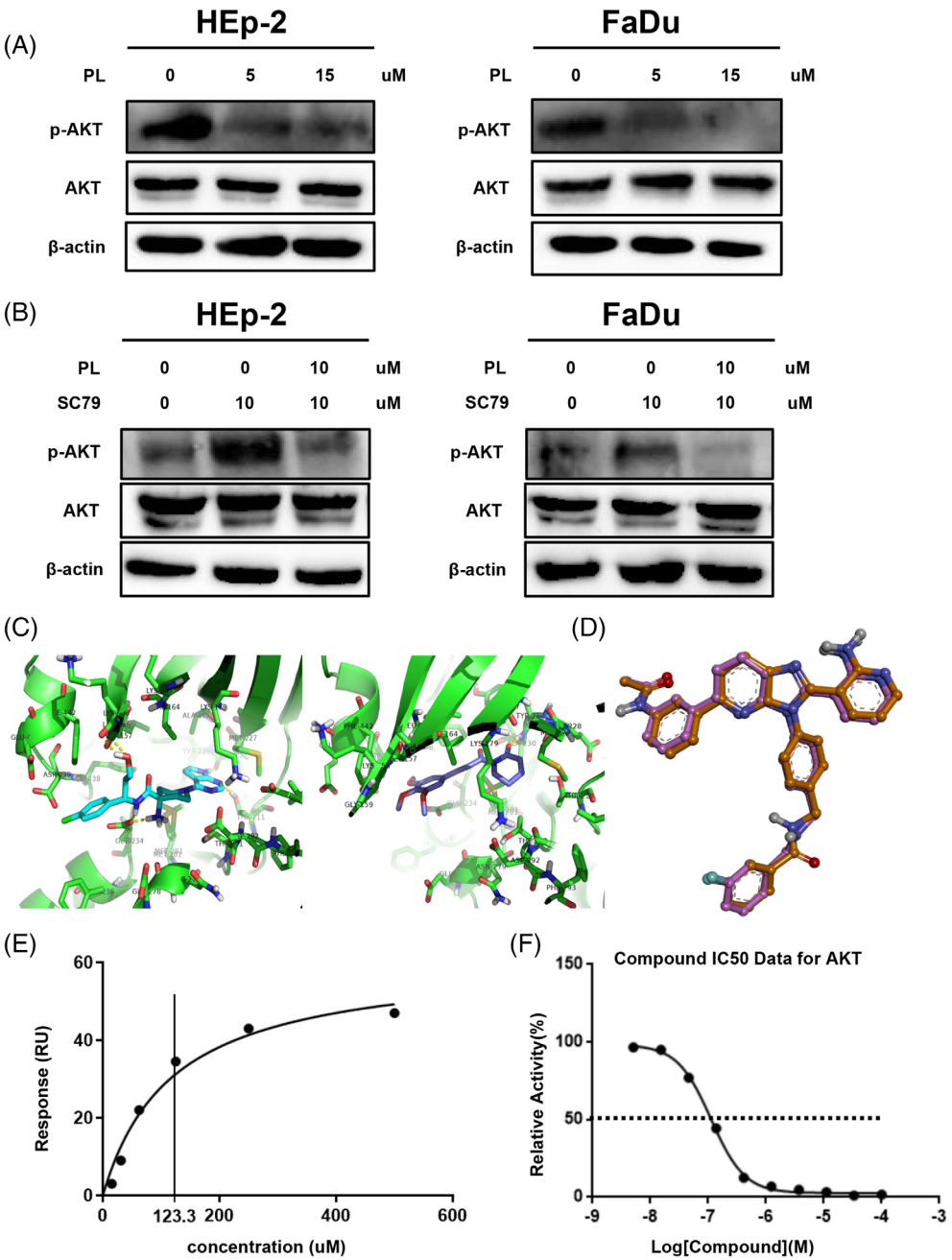

FIGURE 5 Verification of PL targets by molecular docking and western blot. (A) Western blot analysis of total-cell extracts of HNSCC cell lines treated with PL for 24 hr to evaluate the effect of PL on Akt. β-Actin was used as internal control. (B) HEp-2 and FaDu cells were treated with 10 μM of PL for 24 hr. After stimulation with SC79 (Akt activitor, 10 μM) for 1 hr, the cells were harvested and protein levels were measured by western blotting. The extracted protein from two cell lines (n = 2) were measured three times indepently. (C) Visualization by PyMOL of ligand binding with Akt. Left: AZD5363, Right: Pl. (D) Redocking poses of the crystal structure. Green sticks: Experimental pose extracted from X-ray structure. Gray sticks: Docked poses. (E) Biacore analysis results of PL and Akt. The black dot represents various concentrations of PL, PL binds to Akt with a K_D of 123.3 μM. (F) Kinase activity assays were conducted to validate the inhibition of PL on Akt kinase activity. Staurosporine, an effective protein kinase inhibitor, was chosen as positive control [Colour figure can be viewed at wileyonlinelibrary.com]

proteins. However, the real target of PL remains unknown. PL can inhibit HNSCC cell proliferation, promote apoptosis, arrest cell cycle in S phase, and inhibit DNA replication, which is not inferior to cisplatin. Our study suggested that Akt may be the target of PL through online pharmacologic analysis. Activated Akt promotes HNSCC proliferation and metastasis (Georgy et al., 2015), and drugs can inhibit HNSCC metastasis by attenuating Akt activation (Lai et al., 2019). Previous studies have shown that PL can inhibit Akt through PI3K/Akt pathway in a variety of tumors, such as triple negative breast cancer (TNBC) (Kumar & Agnihotri, 2019; Shrivastava et al., 2014). To explore other possible mechanisms by which PL inhibits Akt, molecular docking of PL and Akt crystal were performed. PL and Akt specific inhibitor (AZD5363) can form similar chemical bonds, suggesting that PL can dock to Akt active sites. By redocking poses, the accuracy of the molecular docking was evalueted.

In the biological behavior of tumor cells, proliferation is the most common and important. It has been confirmed in a variety of tumors that knockdown of the PI3K/Akt pathway can inhibit tumor cell proliferation (Fritz, Varga, & Radziwill, 2010). However, the continuous inhibition of PI3K/Akt pathway will result in the decrease of protein activity and therapeutic effect. Therefore, inhibition of Akt can enhance the inhibition of PI3K/Akt pathway. In previous studies, PL inhibited Akt through the PI3K pathway. In this study, we found that PL could also dock to Akt. PI3K-independent inhibition of Akt suggests that PL has multiple inhibitory effects on the PI3K/Akt pathway.

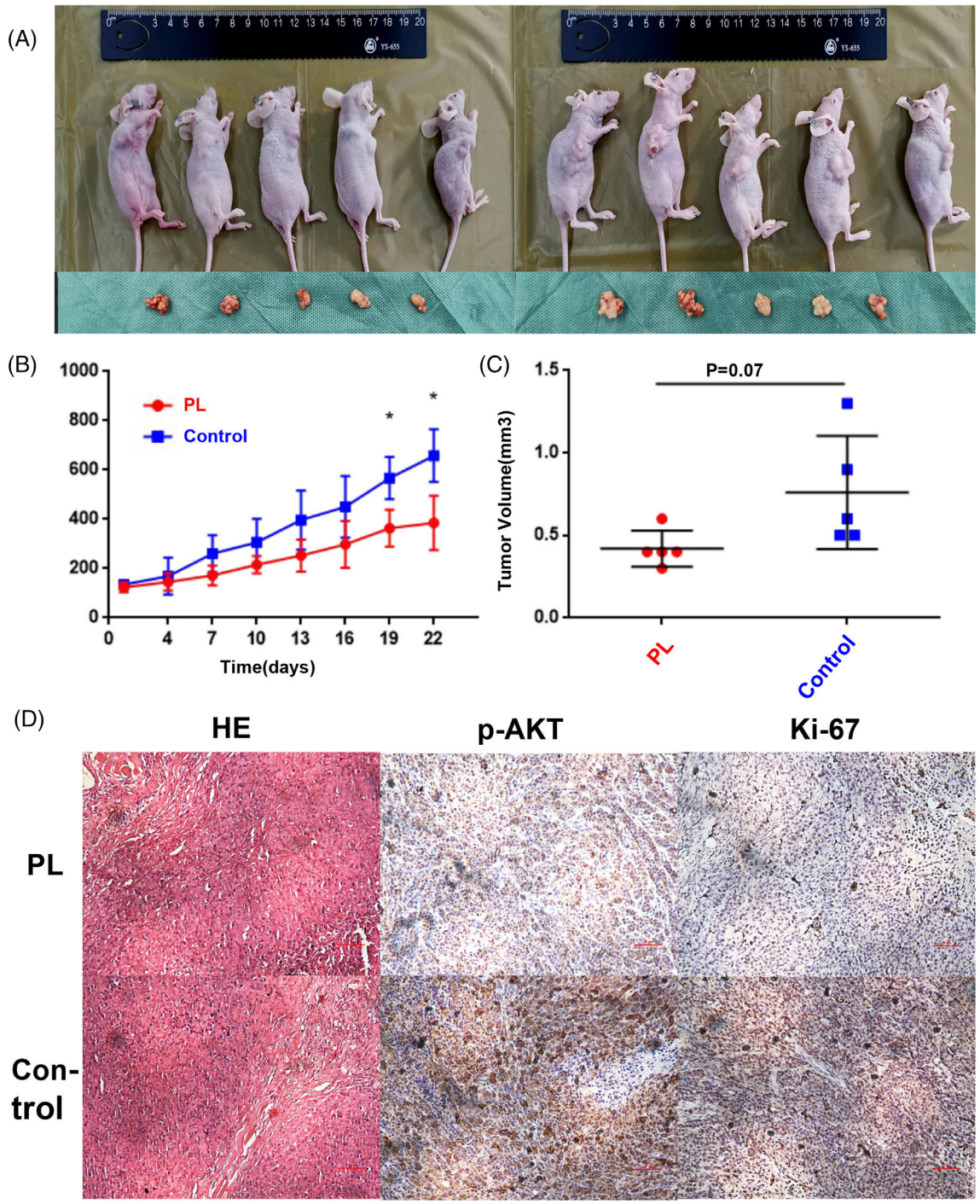

FIGURE 6 PL inhibited HNSCC in vivo. (A) Representative images of tumors generated by PL and saline (left: PL group; right: control group). (B) Tumor volumes were recorded and compared every 2 days. Graph represents tumor volume (in mm^3) over a total of 22 days. (C) Tumor weight was measured at the end of experiment when mice were sacrificed. Graph represents tumor weight (in g) on day 22. Data represent mean ± SD, $^*p < .05$, $n = 5$. (D) Immunohistochemical staining to analyze expression of p-Akt and Ki-67 in tumors [Colour figure can be viewed at wileyonlinelibrary.com]

5 | CONCLUSION

In summary, in this study, we found in vitro and in vivo that PL, a natural ingredient drug, can inhibit the proliferation of laryngeal and hypopharyngeal cancer by docking to Akt. There are some limitations in this study. The conclusions of this study come from cell and animal experiments, and clinical trials are the gold standard to test the efficacy of drugs. We expect to have the clinical trials of PL to provide more drug choices for patients.

ACKNOWLEDGEMENTS

We would like to appreciate the China Medical University Animal Experiment Center for providing facilities and support to in vivo experiment.

CONFLICT OF INTEREST

The authors all declare that they have no conflict of interest.

AUTHOR CONTRIBUTIONS

Xu Ji and Ye Zhang designed the study. Fei Lv conducted experiments, collated data and wrote manuscripts. Jin Bai, Jian Wang and Hong Li provided assistance in bioinformatics, molecular docking and cell culture, respectively. Mingming Deng and Dan Zou revised the manuscript.

DATA AVAILABILITY STATEMENT

The datasets used and/or analyzed during the current study are available from the corresponding author on reasonable request.

ETHICAL STATEMENT

All animal experiments were conducted under a protocol approved by the Ethics Committee of the First Affiliated Hospital of China Medical University.

ORCID

Xu Ji https://orcid.org/0000-0002-7000-7545

REFERENCES

Ashburner, M., Ball, C. A., Blake, J. A., Botstein, D., Butler, H., Cherry, J. M., … Sherlock, G. (2000). Gene ontology: Tool for the unification of biology. The gene ontology consortium. *Nature Genetics*, *25*(1), 25–29.

Ashwell, M. A., Lapierre, J. M., Brassard, C., Bresciano, K., Bull, C., Cornell-Kennon, S., … Chan, T. C. K. (2012). Discovery and optimization of a series of 3-(3-phenyl-3H-imidazo[4,5-b]pyridin-2-yl)pyridin-2-amines: Orally bioavailable, selective, and potent ATP-independent Akt inhibitors. *Journal of Medicinal Chemistry*, *55*(11), 5291–5310.

Bhutani, J., Sheikh, A., & Niazi, A. K. (2013). Akt inhibitors: Mechanism of action and implications for anticancer therapeutics. *Infectious Agents and Cancer*, *8*(1), 49.

Bostan, M., Petrica-Matei, G. G., Ion, G., Radu, N., Mihaila, M., Hainarosie, R., … Neagu, M. (2019). Cisplatin effect on head and neck squamous cell carcinoma cells is modulated by ERK1/2 protein kinases. *Experimental and Therapeutic Medicine*, *18*(6), 5041–5051.

Burley, S. K., Berman, H. M., Bhikadiya, C., Bi, C., Chen, L., Di Costanzo, L., … Zardecki, C. (2019). RCSB protein data Bank: Biological macromolecular structures enabling research and education in fundamental biology, biomedicine, biotechnology and energy. *Nucleic Acids Research*, *47*(D1), D464–D474.

Calleja, V., Alcor, D., Laguerre, M., Park, J., Vojnovic, B., Hemmings, B. A., … Larijani, B. (2007). Intramolecular and intermolecular interactions of protein kinase B define its activation in vivo. *PLoS Biology*, *5*(4), e95.

Cancer Genome Atlas Network. (2015). Comprehensive genomic characterization of head and neck squamous cell carcinomas. *Nature*, *517*(7536), 576–582.

Chen, D., Ma, Y., Li, P., Liu, M., Fang, Y., Zhang, J., … Yin, Y. (2019). Piperlongumine induces apoptosis and synergizes with doxorubicin by inhibiting the JAK2-STAT3 pathway in triple-negative breast cancer. *Molecules*, *24*(12), 2338.

Chen, W., Lian, W., Yuan, Y., & Li, M. (2019). The synergistic effects of oxaliplatin and piperlongumine on colorectal cancer are mediated by oxidative stress. *Cell Death & Disease*, *10*(8), 600.

Davies, B. R., Greenwood, H., Dudley, P., Crafter, C., Yu, D. H., Zhang, J., … Pass, M. (2012). Preclinical pharmacology of AZD5363, an inhibitor of AKT: Pharmacodynamics, antitumor activity, and correlation of monotherapy activity with genetic background. *Molecular Cancer Therapeutics*, *11*(4), 873–887.

Davis, A. P., Murphy, C. G., Saraceni-Richards, C. A., Rosenstein, M. C., Wiegers, T. C., & Mattingly, C. J. (2009). Comparative Toxicogenomics database: A knowledgebase and discovery tool for chemical-gene-disease networks. *Nucleic Acids Research*, *37*, D786–D792.

Dubal, P. M., Unsal, A. A., Echanique, K. A., Vazquez, A., Reder, L. S., Baredes, S., & Eloy, J. A. (2016). Laryngeal adenosquamous carcinoma: A population-based perspective. *Laryngoscope*, *126*(4), 858–863.

Farooqi, A. A., Attar, R., Yaylim, I., Qureshi, M. Z., Todorovska, M., Karatoprak, G. S., … Lin, X. (2018). Piperlongumine as anticancer agent: The story so far about killing many birds with one stone. *Cellular and Molecular Biology (Noisy-le-Grand, France)*, *64*(11), 102–107.

Friesner, R. A., Banks, J. L., Murphy, R. B., Halgren, T. A., Klicic, J. J., Mainz, D. T., … Shenkin, P. S. (2004). Glide: A new approach for rapid, accurate docking and scoring. 1. Method and assessment of docking accuracy. *Journal of Medicinal Chemistry*, *47*(7), 1739–1749.

Fritz, R. D., Varga, Z., & Radziwill, G. (2010). CNK1 is a novel Akt interaction partner that promotes cell proliferation through the Akt-FoxO signalling axis. *Oncogene*, *29*(24), 3575–3582.

Garcia-Carracedo, D., Villaronga, M. A., Alvarez-Teijeiro, S., Hermida-Prado, F., Santamaria, I., Allonca, E., … García-Pedrero, J. M. (2016). Impact of PI3K/AKT/mTOR pathway activation on the prognosis of patients with head and neck squamous cell carcinomas. *Oncotarget*, *7*(20), 29780–29793.

Georgy, S. R., Cangkrama, M., Srivastava, S., Partridge, D., Auden, A., Dworkin, S., … Darido, C. (2015). Identification of a novel proto-oncogenic network in head and neck squamous cell carcinoma. *Journal of the National Cancer Institute*, *107*(9), djv152.

Gong, L. H., Chen, X. X., Wang, H., Jiang, Q. W., Pan, S. S., Qiu, J. G., … Yan, X.-J. (2014). Piperlongumine induces apoptosis and synergizes with cisplatin or paclitaxel in human ovarian cancer cells. *Oxidative Medicine and Cellular Longevity*, *2014*, 906804.

Gu, S. M., Lee, H. P., Ham, Y. W., Son, D. J., Kim, H. Y., Oh, K. W., … Hong, J. T. (2018). Piperlongumine improves lipopolysaccharide-induced Amyloidogenesis by suppressing NF-KappaB pathway. *Neuromolecular Medicine*, *20*(3), 312–327.

Halgren, T. A., Murphy, R. B., Friesner, R. A., Beard, H. S., Frye, L. L., Pollard, W. T., & Banks, J. L. (2004). Glide: A new approach for rapid, accurate docking and scoring. 2. Enrichment factors in database screening. *Journal of Medicinal Chemistry*, *47*(7), 1750–1759.

Han, S. S., Han, S., & Kamberos, N. L. (2014). Piperlongumine inhibits the proliferation and survival of B-cell acute lymphoblastic leukemia cell lines irrespective of glucocorticoid resistance. *Biochemical and Biophysical Research Communications*, *452*(3), 669–675.

Han, S. S., Son, D. J., Yun, H., Kamberos, N. L., & Janz, S. (2013). Piperlongumine inhibits proliferation and survival of Burkitt lymphoma in vitro. *Leukemia Research*, *37*(2), 146–154.

Huang, D. W., Sherman, B. T., & Lempicki, R. A. (2009). Systematic and integrative analysis of large gene lists using DAVID bioinformatics resources. *Nature Protocols*, *4*(1), 44–57.

Hutchinson, L. (2016). Drug therapy: Cetuximab or cisplatin in HNSCC? *Nature Reviews. Clinical Oncology*, *13*(2), 66.

Ippen, F. M., Grosch, J. K., Subramanian, M., Kuter, B. M., Liederer, B. M., Plise, E. G., … Brastianos, P. K. (2019). Targeting the

PI3K/Akt/mTOR pathway with the pan-Akt inhibitor GDC-0068 in PIK3CA-mutant breast cancer brain metastases. *Neuro-Oncology*, *21*(11), 1401–1411.

Jiang, B. H., & Liu, L. Z. (2008). AKT signaling in regulating angiogenesis. *Current Cancer Drug Targets*, *8*(1), 19–26.

Kaidar-Person, O., Gil, Z., & Billan, S. (2018). Precision medicine in head and neck cancer. *Drug Resistance Updates*, *40*, 13–16.

Kanehisa, M., & Goto, S. (2000). KEGG: Kyoto encyclopedia of genes and genomes. *Nucleic Acids Research*, *28*(1), 27–30.

Karki, K., Hedrick, E., Kasiappan, R., Jin, U. H., & Safe, S. (2017). Piperlongumine induces reactive oxygen species (ROS)-dependent downregulation of specificity protein transcription factors. *Cancer Prevention Research (Philadelphia, PA.)*, *10*(8), 467–477.

Ke, Z. B., Cai, H., Wu, Y. P., Lin, Y. Z., Li, X. D., Huang, J. B., … Xu, N. (2019). Identification of key genes and pathways in benign prostatic hyperplasia. *Journal of Cellular Physiology*, *234*(11), 19942–19950.

Kumar, S., & Agnihotri, N. (2019). Piperlongumine, a piper alkaloid targets Ras/PI3K/Akt/mTOR signaling axis to inhibit tumor cell growth and proliferation in DMH/DSS induced experimental colon cancer. *Biomedicine & Pharmacotherapy*, *109*, 1462–1477.

Kuo, P., Sosa, J. A., Burtness, B. A., Husain, Z. A., Mehra, S., Roman, S. A., … Judson, B. L. (2016). Treatment trends and survival effects of chemotherapy for hypopharyngeal cancer: Analysis of the National Cancer Data Base. *Cancer*, *122*(12), 1853–1860.

Lai, Y. J., Yu, W. N., Kuo, S. C., Ho, C. T., Hung, C. M., Way, T. D., & Chen, C. T. (2019). CSC-3436 inhibits TWIST-induced epithelial-mesenchymal transition via the suppression of Twist/Bmi1/Akt pathway in head and neck squamous cell carcinoma. *Journal of Cellular Physiology*, *234*(6), 9118–9129.

Leonard, P., Hearty, S., Ma, H., & O'Kennedy, R. (2017). Measuring protein-protein interactions using Biacore. *Methods in Molecular Biology*, *1485*, 339–354.

Li, Q., Chen, L., Dong, Z., Zhao, Y., Deng, H., Wu, J., … Li, W. (2019). Piperlongumine analogue L50377 induces pyroptosis via ROS mediated NF-kappaB suppression in non-small-cell lung cancer. *Chemico-Biological Interactions*, *313*, 108820.

Liu, J., Liu, W., Lu, Y., Tian, H., Duan, C., Lu, L., … Yang, H. (2018). Piperlongumine restores the balance of autophagy and apoptosis by increasing BCL2 phosphorylation in rotenone-induced Parkinson disease models. *Autophagy*, *14*(5), 845–861.

Liu, Z., Guo, F., Wang, Y., Li, C., Zhang, X., Li, H., … He, F. (2016). BATMAN-TCM: A bioinformatics analysis tool for molecular mechANism of traditional Chinese medicine. *Scientific Reports*, *6*, 21146.

Lu, C., Zhang, B., Xu, T., Zhang, W., Bai, B., Xiao, Z., … Dai, Y. (2019). Piperlongumine reduces ovalbumininduced asthma and airway inflammation by regulating nuclear factorkappaB activation. *International Journal of Molecular Medicine*, *44*(5), 1855–1865.

Massard, C., Gordon, M. S., Sharma, S., Rafii, S., Wainberg, Z. A., Luke, J., … Segal, N. H. (2016). Safety and efficacy of Durvalumab (MEDI4736), an anti-programmed cell death Ligand-1 immune checkpoint inhibitor, in patients with advanced urothelial bladder cancer. *Journal of Clinical Oncology*, *34*(26), 3119–3125.

Mayer, I. A., & Arteaga, C. L. (2016). The PI3K/AKT pathway as a target for cancer treatment. *Annual Review of Medicine*, *67*, 11–28.

Nguyen, C. T., Tanaka, K., Cao, Y., Cho, S. H., Xu, D., & Stacey, G. (2016). Computational analysis of the ligand binding site of the extracellular ATP receptor, DORN1. *PLoS One*, *11*(9), e161894.

Robertson, J., Coleman, R. E., Cheung, K. L., Evans, A., Holcombe, C., Skene, A., … Gee, J. M. W. (2019). Proliferation and AKT activity biomarker analyses after Capivasertib (AZD5363) treatment of patients with ER(+) invasive breast cancer (STAKT). *Clinical Cancer Research*, *26*(7), 1574–1585.

Ru, J., Li, P., Wang, J., Zhou, W., Li, B., Huang, C., … Yang, L. (2014). TCMSP: A database of systems pharmacology for drug discovery from herbal medicines. *Journal of Cheminformatics*, *6*, 13.

Saito, R., Smoot, M. E., Ono, K., Ruscheinski, J., Wang, P. L., Lotia, S., … Ideker, T. (2012). A travel guide to Cytoscape plugins. *Nature Methods*, *9*(11), 1069–1076.

Seber, J., Sirin, D. Y., Yetisyigit, T., & Bilgen, T. (2020). Piperlongumine increases the apoptotic effect of doxorubicin and paclitaxel in a cervical cancer cell line. *Nigerian Journal of Clinical Practice*, *23*(3), 386–391.

Seok, J. S., Jeong, C. H., Petriello, M. C., Seo, H. G., Yoo, H., Hong, K., & Han, S. G. (2018). Piperlongumine decreases cell proliferation and the expression of cell cycle-associated proteins by inhibiting Akt pathway in human lung cancer cells. *Food and Chemical Toxicology*, *111*, 9–18.

Shrivastava, S., Kulkarni, P., Thummuri, D., Jeengar, M. K., Naidu, V. G., Alvala, M., … Ramakrishna, S. (2014). Piperlongumine, an alkaloid causes inhibition of PI3 K/Akt/mTOR signaling axis to induce caspase-dependent apoptosis in human triple-negative breast cancer cells. *Apoptosis*, *19*, 1148–1164.

Simon, C., & Caballero, C. (2018). Quality assurance and improvement in head and neck cancer surgery: From clinical trials to National Healthcare Initiatives. *Current Treatment Options in Oncology*, *19*(7), 34.

Steuer, C. E., El-Deiry, M., Parks, J. R., Higgins, K. A., & Saba, N. F. (2017). An update on larynx cancer. *CA: A Cancer Journal for Clinicians*, *67*(1), 31–50.

Thongsom, S., Suginta, W., Lee, K. J., Choe, H., & Talabnin, C. (2017). Piperlongumine induces G2/M phase arrest and apoptosis in cholangiocarcinoma cells through the ROS-JNK-ERK signaling pathway. *Apoptosis*, *22*(11), 1473–1484.

Wang, F., Mao, Y., You, Q., Hua, D., & Cai, D. (2015). Piperlongumine induces apoptosis and autophagy in human lung cancer cells through inhibition of PI3K/Akt/mTOR pathway. *International Journal of Immunopathology and Pharmacology*, *28*(3), 362–373.

Wang, H., Wang, Y., Gao, H., Wang, B., Dou, L., & Li, Y. (2018). Piperlongumine induces apoptosis and autophagy in leukemic cells through targeting the PI3K/Akt/mTOR and p38 signaling pathways. *Oncology Letters*, *15*(2), 1423–1428.

Wang, S. H., & Yu, J. (2018). Structure-based design for binding peptides in anti-cancer therapy. *Biomaterials*, *156*, 1–15.

Xue, K., Wang, Y. N., Zhao, X., Zhang, H. X., Yu, D., & Jin, C. S. (2019). Synergistic effect of meta-tetra(hydroxyphenyl)chlorin-based photodynamic therapy followed by cisplatin on malignant Hep-2 cells. *Oncotargets and Therapy*, *12*, 5525–5536.

Xue, R., Fang, Z., Zhang, M., Yi, Z., Wen, C., & Shi, T. (2013). TCMID: Traditional Chinese medicine integrative database for herb molecular mechanism analysis. *Nucleic Acids Research*, *41*, D1089–D1095.

Yadav, D. K., Dhawan, S., Chauhan, A., Qidwai, T., Sharma, P., Bhakuni, R. S., … Khan, F. (2014). QSAR and docking based semi-synthesis and in vivo evaluation of artemisinin derivatives for antimalarial activity. *Current Drug Targets*, *15*(8), 753–761.

Yadav, D. K., Kalani, K., Khan, F., & Srivastava, S. K. (2013). QSAR and docking based semi-synthesis and in vitro evaluation of 18 beta-glycyrrhetinic acid derivatives against human lung cancer cell line A-549. *Medicinal Chemistry*, *9*(8), 1073–1084.

Yadav, D. K., Kalani, K., Singh, A. K., Khan, F., Srivastava, S. K., & Pant, A. B. (2014). Design, synthesis and in vitro evaluation of 18beta-glycyrrhetinic acid derivatives for anticancer activity against human breast cancer cell line MCF-7. *Current Medicinal Chemistry*, *21*(9), 1160–1170.

Yamaguchi, Y., Kasukabe, T., & Kumakura, S. (2018). Piperlongumine rapidly induces the death of human pancreatic cancer cells mainly through the induction of ferroptosis. *International Journal of Oncology*, *52*(3), 1011–1022.

Zhou, J., Huang, Z., Ni, X., & Lv, C. (2020). Piperlongumine induces apoptosis and G2/M phase arrest in human osteosarcoma cells by regulating ROS/PI3K/Akt pathway. *Toxicology in Vitro*, *65*, 104775.

Zhu, J. L., Wu, Y. Y., Wu, D., Luo, W. F., Zhang, Z. Q., & Liu, C. F. (2019). SC79, a novel Akt activator, protects dopaminergic neuronal cells

from MPP(+) and rotenone. *Molecular and Cellular Biochemistry*, *461*, 81–89.

SUPPORTING INFORMATION

Additional supporting information may be found online in the Supporting Information section at the end of this article.

How to cite this article: Lv F, Deng M, Bai J, et al. Piperlongumine inhibits head and neck squamous cell carcinoma proliferation by docking to Akt. *Phytotherapy Research*. 2020;1–14. https://doi.org/10.1002/ptr.6788